Closed circuit PRO series No 4: CC-PRO hydroelectric power generation prospects from the Red Sea brine and Dead Sea salinity gradient

Avi Efraty*

Osmotech Ltd, P.O. Box 132, 90836 Har Adar, Israel, Tel. +972 52 4765 687; Fax: +972 2 570 0262;
email: efraty.adt@012.net.il (A. Efraty)

ABSTRACT

The Red Sea (RS) to Dead Sea (DS) water transfer project in Jordan under the sponsorship of the World Bank is intended to stop the sea-level decline of the DS as well as for the desalination of RS water and for hydroelectric power generation. Red Sea Brine (RSB ~7.13%) disposal to the DS (~34%) creates a salinity gradient of interest for PRO hydroelectric power generation and the prospects of such an application are explored in the present study with the most advanced existing tools including a new Closed Circuit PRO technology (CC-PRO) of near absolute energy efficiency without need of ERD and a recent PRO membrane (HTI-TFC) of the highest reported strength to withstand applied pressure up to 48.3 bar. Power generation prospects from RSB–DS using CC-PRO with HTI-TFC are assessed in the actual/ideal flux ratio (β) range 0.123–0.400 and High Salinity Feed (DS as draw solution) to permeation flow ratio (δ) range 1–25. The minimum $\beta = 0.123$ for said process is established from available PRO experimental data with HTI-TFC for 0.6–3.0 M NaCl salinity gradients accounting for the presence of considerable concentrations of divalent cations such as Ca and Mg in DS water. The Net Electric Power (NEP) generation prospects from the RSB–DS Jordanian project using CC-PRO and HTI-TFC are assessed on the basis of 120 Mm^3/year RSB availability for mixing with DS water. The results of this study accounting for the pressure limitation of HTI-TFC reveal NEP generation prospects of 7,753 kW under the conditions of $\delta = 1.0$ and $\beta = 0.123$-0.200 from the RSB–DS gradient, or a supplement of 56.6% more power on top of the conventional hydroelectric power generation facility of the project (~13,698 kW). If the HTI-TFC membrane, or alike, could be made to operate at maximum PRO pressures of 60 and 86 bar, the CC-PRO NEP availability from RSB–DS is expected to rise to 9,767 kW (71.3%) and 13,219 kW (96.5%), respectively, with added power to the project indicated in parenthesis. In simple terms, the current state of the art revealed in this study suggest the immediate availability of the CC-PRO technology with HTI-TFC membranes for economical NEP generation from the RSB–DS gradient in the context of the Jordanian project with future improvements of membranes to withstand higher applied pressures expected to improve the economic feasibility.

Keywords: Forward osmosis; Osmotic power; Salinity gradient power; Pressure-retarded osmosis (PRO); Closed circuit PRO; Clean energy sources; Red Sea; Dead Sea

1. Introduction

The application of pressurized permeation flow across semi-permeable membranes by solutions of different salinity for hydroelectric power generation was conceived in 1975 by Loeb [1–5] and termed by him "pressure-retarded osmosis" (PRO). This invention was inspired by the Israeli plan to connect the Mediterranean to the Dead Sea (DS ~400 m below Mediterranean sea level) for hydroelectric power generation and Loeb, the co-inventor [6] of reverse osmosis (RO) desalination 15 year earlier, was aware of the enormous osmotic pressure difference (>200 bar) between these two water sources and this led to the inception of the membrane-based PRO technology with an energy recovery device (ERD) for hydroelectric power generation from salinity gradients. Early PRO experiments with DS water were not particularly encouraging and led to the article [5] entitled "Energy production at the Dead Sea by pressure-retarded osmosis: challenge or chimera?". Recent advances covering both the PRO technology and membranes, considered hereinafter, demonstrate the immediate economical feasibility of PRO and its future prospects for clean energy generation in large amounts from natural and man-made salinity gradients.

The rapidly growing activities on various PRO aspects over the past few years, covered since 2009 by an increasing number of review-like articles [7–20], created extensive theoretical and experimental knowledge on advanced PRO membranes [21–32] and validated the PRO concept with ERD at the level of demonstration plants in Norway [33–35] and Japan [36–38]. Emphasis in the development and characterization of advance PRO membranes focused on new generations of fabricated PRO membranes of reduced detrimental effects with increased mechanical strength to withstand higher applied pressures of greater power density availability. In order to enable effective PRO performance of advance membranes, it was also necessary to upgrade the PRO technology in order to allow the attainment of high energy conversion efficiency since experience gained with ERD in modern advanced sea water desalination plants revealed energy conversion efficiency of 76% [39] or less [40] not sufficient to sustain an economically viable PRO process. A recent development of the closed circuit PRO (henceforth "CC-PRO") technology [41–43] of near absolute energy efficiency without ERD together with advanced PRO membranes is expected to open the door for the first time to PRO of economic feasibility and this aspect is demonstrated in the current study.

The CC-PRO technology is illustrated schematically in Fig. 1(A–B) with a single module apparatus

comprising either one or two side conduits (SCs) with valve means for engagement or disengagement with a closed circuit PRO system. The function of the engaged SC is to supply pressurized high salinity feed (henceforth "HSF" or draw) to module's inlet and retrieve high salinity diluted feed (henceforth "HSDF" or diluted draw) from its outlet. Replacement of HSDF by HSF takes place in the disengaged decompressed SC and the entire process is of near absolute energy efficiency since the compression/decompression steps are carried out hydrostatically with negligible amounts of the internally created PRO energy. Noteworthy features of the CC-PRO technology include HSF flow control at inlet to module by means of CP
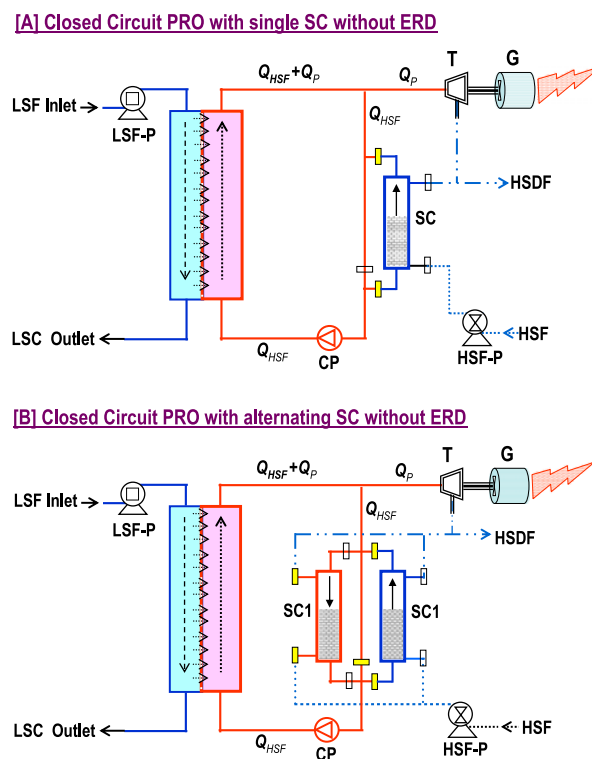

Fig. 1 (A–B). Schematic designs of a single module CC-PRO apparatus of one (A) and two (B) side-conduit configurations. Abbreviations: LSP, Low Salinity Feed ("feed" solution); LSC, Low Salinity Concentrated (concentrated "feed" effluent); HSF, High Salinity Feed ("draw" solution); HSDF, High Salinity Diluted Feed (diluted "draw" solution); T, Turbine; G, Generator; HSF-P, High Salinity Feed Pump; LSP-P Low Salinity Feed Pump; CP, Circulation Pump; SC, Side Conduit; small rectangles symbolize actuated valve means except for HSF inlets to SCs where one-way check valves are used instead of actuated valves; Q stands flow rates of cited components with Q_p pertaining to permeation flow across the semi-permeable membrane; **red** color symbolizes pressurized sections and **blue** color non-pressurized sections in the apparatus.

($Q_{CP} = Q_{HSF} = Q_{draw}$) whereby PRO can be carried out with a selected HSF/Permeation flow ratio ($\delta = Q_{CP}/Q_P = Q_{HSF}/Q_P = Q_{draw}/Q_P$) of the desired stationary state conditions for maximum Net Electric Power (henceforth "NEP") generation which takes into account the membrane power density, the efficiency of turbine-generator (T-G), and the power consumption of the auxiliary pump (CP, HSF-P, and LSF-P) in the design (Fig. 1(A–B)). The selected flow ratio δ of defined module stationary state conditions also implies operation with a fixed percent (α) permeate in HSDF expressed by $\alpha = 100 \times Q_P/Q_{HSDF} = 100 \times Q_P/(Q_{HSF} + Q_P) = 100/(\delta + 1)$. The conventional PRO demonstration pilot in Japan was reported [38] to operate at $\alpha = 40\%$ ($\delta = 1.5$) with an ultimate stated goal to reach $\alpha = 60\%$ ($\delta = 0.667$). CC-PRO is the only known technology available today for PRO hydroelectric power generation of near absolute energy efficiency without need of ERD and this implies 20–45% greater NEP output compared with the conventional PRO technique depending on the efficiency of its ERD.

The present study explores the prospects for NEP generation with CC-PRO from the salinity gradient of Red Sea brine (RSB) and Dead Sea (DS) sources using the recently reported [32] HTI-TFC membrane of the highest presently known operational pressure (48.3 bar–700 psi). The salinity gradient under consideration is expected in the Red Sea (RS) to Dead Sea water transfer project [44] about to start in Jordan by the sponsorship of the World Bank. This pilot project involves the construction of a 80 Mm^3/y (219,178 m^3/d) SWRO desalination plant of 40% recovery to be fed by 200 Mm^3/year of RS (~4.28%) water which will produce 120 Mm^3/y RSB (~7.13%) for disposal in the DS (~34%) through a hydroelectric power generation system exploiting the 400 m height difference. This project will make available a salinity gradient system (RSB–DS) of near 200 bar osmotic pressure difference on the shores of the DS and thereby provide an exception site for the development of a major PRO application of considerable economic prospects and an added benefit to the RS–DS pilot project. The pilot project is expected to lead to a 10-fold larger program whose ultimate goals are to stop the rapidly declined DS level (−420 m) and at the same time generate hydroelectric power and provide desalinated seawater in an arid zone of great demand for fresh water. Adding a CC-PRO step to the Jordanian pilot project and program assessed herein could imply a major hydroelectric power supplement as bonus without altering existing plans just by utilizing the RSB effluent at entry point to the DS.

This study is part of a series intended for the evaluation of hydroelectric power generation prospects from different salinity gradient sources with the CC-PRO technology. The Jordanian RS–DS water transfer project provides a unique opportunity to test a salinity gradient of high osmotic pressure difference for large-scale PRO hydroelectric power generation as an added benefit and thereby justify enormous efforts by many [7−20] for the making of this noteworthy approach useful for clean energy generation worldwide.

2. Power generation prospects of CC-PRO with HTI-TFC on the basis of β-A analysis.

The investigated membrane by Straub et al. [32] is an ordinary flat-sheet thin-film composite (TFC) forward osmosis (FO) membrane ($A = 2.49$ lmh/bar; $B = 0.39$ lmh and $S = 564$ μm) from Hydration Technology Innovation (HTI) [45] made of a polyamide active layer and designed to withstand pressure up to 700 psi (48.3 bar). Reported [32] PRO flux as function of hydraulic pressure difference for the salinity gradients 0.6; 1.0; 2.0; and 3.0 M NaCl made it possible to extrapolate the actual FO flux (40; 42; 53; and 59 lmh), ideal flux (A*$\Delta\pi$: 70.2; 123.0; 276.6; and 470.1 lmh), and actual/ideal flux ratio (β) terms (0.57; 0.341; 0.191; and 0.123), respectively. The power density projection curves of the HTI-TFC membrane as function of molar NaCl concentration in Fig. 2(A–D) are derived by the application of the β terms in the context of the actual flux (J_a − lmh) expression Eq. (1) and the actual power density expression Eq. (2); wherein, p (bar) stands for hydraulic pressure difference or the applied pressure of hydroelectric power generation, $\Delta\pi_i$ for osmotic pressure difference at module inlet, and W(w/m^2) for the projected power density of the membrane. The β-A-based power density projection curves in Fig. 2(A–D) for HTI-TFC show good agreement with the experimental results reported [32] by Straub et al. and are consistent with similar findings for other PRO membranes [46]. Since β is the actual/ideal flux ratio under FO conditions, the correlations between the β-A power density projection curves and the experimental results over the wide ranges of applied pressures and salinity gradients displayed in Fig. 2(A–D) imply similar detrimental effects on flux in both FO and PRO of strong dependence on the permeability coefficient (A) and module inlet salinity gradient manifested by $\Delta\pi_i$. It should be pointed out that the correlation between β-A power density projections and experimental results revealed in Fig. 2(A–D) are said for high HSF/Permeate flow ratio ($\delta > 25$) of low percent ($\alpha < 4\%$) permeate in HSDF typical of stationary state conditions inside PRO modules of small concentration difference between inlet and outlet which are of low practical plausibility for power exploitation.
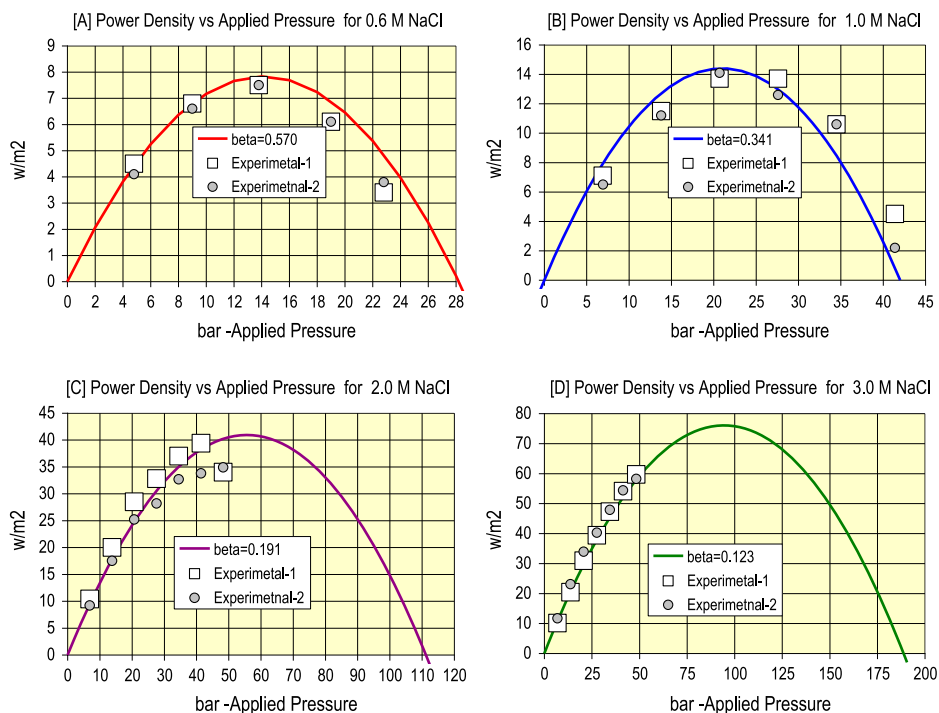
Fig. 2 (A–D). The β-A power density projection curves for the HTI-TFC membrane in various NaCl salinity gradients as function of applied pressures compared with reported [32] experimental results.

$$J_a = \beta * A * (\Delta\pi_i - p) \tag{1}$$

$$W = (1/36) * J_a * p = (1/36) * \beta * A * (\Delta\pi_i - p) * p \tag{2}$$

The correlation between β and the molar concentrations of NaCl for the HTI-TFC membrane in Fig. 3 shows an exponentially declined β with increased module inlet concentration and this most probably reflects a strong reverse salt flux effect on β as
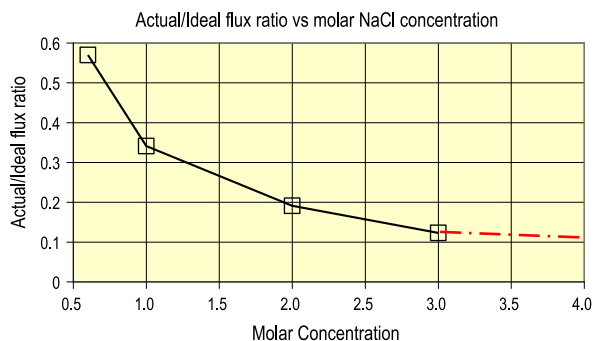

Fig. 3. Actual/ideal flux ratio for the HTI-TFC membrane as function of molar NaCl concentration according to the data in Fig. 2(A–D).

function of the salt diffusion coefficient (B) and the initial molar concentration.

The data in Fig. 3 also suggest a limiting β value at high molar concentration (>3M NaCl) in the actual/ideal ratio range 0.10–0.11. Reverse salt flux from HSF (draw) to LSF (feed) is known to reduce the PRO osmotic driving force and effects declined membrane efficiency. Reverse salt flux effect on PRO osmotic driving force is particularly pronounced in case of HSF comprising mono-valence anions due to their distinctly higher reverse salt flux selectively compared with divalent anions. In HSF to PRO comprising both single and divalent anions, the reverse salt diffusion of the counter ions associated with the divalent anions is also confined due to neutral charge balance requirements.

The intent of the aforementioned is to assess the plausibility of the HTI-TFC membrane for CC-PRO power generation in the context of the RSB–DS salinity gradient with expected $\Delta\pi \approx 220$ bar in the range defined by 3–4 M NaCl solutions in Fig. 3. DS water comprises relatively high concentrations of divalent cations (Mg and Ca) with negligible amounts of sulfate (SO_4) and drawing analogy with the referred NaCl solutions in Fig. 3 would suggest a minimum actual/ideal flux ratio $\beta = 0.123$ for HTI-TFC with CC-PRO in the context of RSB–DS with a reasonable expectation for

a significantly higher β value in light of the relatively high divalent ions composition of the DS.

3. Power generation prospects from RSB–DS using CC-PRO with HTI-TFC (A = 2.49 lmh/bar) at δ = 10 assuming β = 0.123

The theoretical model simulation data base for CC-PRO already disclosed elsewhere [43] is considered hereinafter in the context of the RSB–DS salinity gradient with the HTI-TFC membrane of the assumed actual/ideal flux ratio (henceforth "flux ratio") β = 0.123 as minimum. The simulation database in Table 1 pertains to CC-PRO power generation operation in the salinity gradient system comprising DS surface water of 34%(w/v) and RSB of 7.13%(w/v) of $\Delta\pi_i \approx 220$ bar with the HTI-TFC membrane of a defined permeability coefficient (A = 2.49 lmh/bar) at an assumed β = 0.123 minimum flux ratio under module stationary state conditions created by the HSF/Permeate flow ratio (henceforth "flow ratio") δ = 10 of α = 9.09% permeate in HSDF. The power generation prospects as function of applied pressure under the stationary state conditions defined in Table 1 are displayed in Fig. 4 with a vertical line at 49.3 bar revealing the power components for the HTI-TFC membrane maximum pressure limit. Noteworthy features in the simulation database displayed in Table 1 include module inlet, outlet and average concentrations, osmotic pressures, flux, Net Driving Pressures (NDP), and the flow rate terms associated with the CC-PRO process under fixed stationary state conditions with power output defined by A = 2.49 lmh/bar; β = 0.123; δ = 10; α = 9.09%; membrane surface area (42 m^2); and the salinity gradient osmotic pressure difference at module inlet ($\Delta\pi_i$ = 220).

Salinity gradient osmotic pressures of the Red Sea (RS approx: Cl, 55.2; Br, 0.2; SO$_4$, 7.7; HCO$_3$, 0.4; Na, 30.6; K, 1.1; Ca, 1.1; Mg, 3.7% and 42,802 ppm TDS) desalination brine of 40% recovery (RSB approx: 71,337 ppm TDS) and the Dead Sea surface water (DS approx: Cl, 66.1; Br, 1.5; SO$_4$, 0.2; HCO$_3$ 0.1; Na, 11.8; K, 2.3; Ca, 5.1; Mg, 12.9%; and 340,038 ppm TDS) [44] in Table 1 are derived by the van't Hoff equation $\pi = (i/V_m)nRT$; wherein, i stands for dimensionless factor, V_m for volume of pure solvent, n for number of solute molecules, R for ideal gas constant, and T for absolute temperature. The conversion factors [$\Delta\pi$(bar)/C(%)] used in the CC-PRO simulation manifest the cited concentrations and van't Hoff osmotic pressures of the RSB–DS constituents. The NaCl contents of RS (~77.6%) and DS (~30.3%) reveal large variations from pure NaCl solutions (100% NaCl) and their osmotic pressures even at high concentrations are not expected to deviate by much from the van't Hoff equation. The value β = 0.123 in Table 1 is the minimum expected flux ratio in said salinity gradient derived by analogy with the end range data for the same membrane in 3–4 M NaCl gradients (Fig. 3) after accounting for the presence of considerable amounts of divalent ions in DS surface water (5.5% Ca and 12.9% Mg) which should effect a lower reverse salt flux and therefore, a higher β term compared with that of pure NaCl of similar molar concentrations. The database in Table 1 takes account of the calcium and sulfate contents of the RSB (approx: SO$_4$, 5,492 ppm and Ca, 784 ppm) and the intent of the selected flow ratio LSC/LSF = 0.5 is to avoid calcium sulfate scaling during the process. NEP, the single most important product of CC-PRO, specified in Table 1 takes full account of the power consumption of the auxiliary pumps (Fig. 1: CP, LSF-P, and HSF-P) with flow rates of pumps derived directly from the simulated performance data and their pressure of operation and efficiency terms assumed. The selected operational pressure difference for CP assumes a module design of low flow friction-induced pressure losses.

PRO power curves as function of applied pressure per fixed A and β coefficients are generated automatically by the CC-PRO simulation program for a selection flow ratio (δ) of defined stationary state conditions inside the PRO module by dictating the inlet and outlet concentrations, osmotic pressure, and flow rates. The power density dependence on applied pressure in Fig. 4 for RSB-DS with HTI-TFC is based on δ = 10 selection of α = 9.09% with assumed A = 2.49 lmh/bar and β = 0.123 flux ratio. If the A and β coefficients remain unchanged, each δ selection will give rise to a different power curve due to change of the stationary state conditions inside the PRO module. Plugging a selected applied pressure into the simulation database in Table 1 and adjusting for the newly created average actual flux at the bottom right-hand side of the table will generate all the specific power and energy parameters of the system per said applied pressure. In this context, the specific power data in Table 1 relates to peak power density (64.4 W/m^2) at peak pressure (88 bar) and its turbine-generator derivative (58.0 W/m^2) displayed in Fig. 4 as well as a different peak power density of NEP (47.2 W/m^2) at 96 bar due to the incorporation of the power consumption parameters of the auxiliary pumps. The distinction between the membrane power and NEP availability is rather important since the latter determines the economic feasibility by showing the energy made available to customers. Peak power operation of

Table 1
Theoretical power generation prospects from the RSB–DS salinity gradient using CC-PRO with HTI-TFC membrane ($A = 2.49$ lmh/bar) of an assumed $\beta = 0.123$ as minimum illustrating performance under stationary state conditions defined by $\delta = 10$ of $\alpha = 9.09\%$ showing membrane peak power density of 64.4 W/m² at 88 bar applied pressure of 47.2 W/m² NEP availability

34.0	% w/v DS	272.0 bar OP
7.13	% w/v RSB	52.05 bar OP
		220.0 bar Δπ

Design & Membrane Data

1	Number of Modules
1	No of Membrans per Module
205	cm length of module
30	cm, inner diameter of module
145	liter, gross volume of module
50.0	% membrane volume in module*
72.4	liter net volume of Module
42.0	m2, membrane surface per module
42.0	m2 total surface area of design

LSF-LSC Performance Data

Module	Unit		
2.22	2.22	m3/h	LSF Inlet Flow
7.13	7.13	%	LSF inlet Salinity
1.11	1.11	m3/h	LSC outlet Flow
14.26	14.26	%	LSC outlet Salinity
1.11	1.11	m3/h	Permeation Flow
10.70	10.70	%	mean Salinity (inlet+outlet)/2
85.56	85.56	bar	mean Δπ (inlet+outlet)/2
0.50	0.50		Ratio Q_{LSC}/Q_{LSF} $Q_p = Q_{LSF} - Q_{LSC}$
50	50		**% permeate from LSF**

8.00	Δπ(bar)/C(%) - HSF at inlet
8.00	Δπ(bar)/C(%) - HSDF at outlet
7.30	Δπ(bar)/C(%) - LSF & LSC average

PRO Membranes Detrimental Effect

0.123	Ratio Actual/Ideal*
87.7	**% Detrimental Effects**

Fixed Flux per Single Module

26.4	lmh Flux (Selected average)
1.11	m3/h (Q_p) Module average Permeate
18.48	lpm Module average Permeate

Recycled Flow (CP) of Single Module

11.09	m3/h recycling flow (Q_{CP})
184.8	lpm recycling flow (Q_{CP})
0.39	minute complete volume recycle
10.00	Selected Flow Ratio (Q_{CP}/Q_p)
0.392	**min, HSF residence in module**

Flow of Entire Design

1.11	m3/h Permeate Flow of entire unit
11.09	m3/h Recycling Flow of entire unit
9.09	**% permeate in HSDF**

HSF - HSDF Module Inlet & Outlet Data

34.0	% HSF Module Inlet
215.0	bar Δπ Module Inlet
30.9	% HSDF Module Outlet
133.2	bar Δπ Module Outlet
32.5	% HSDF average
174.1	bar Δπ Module average

Power Demand of CC-PRO PUMPS

Performance	HSP	LSP	CP
m3/h	11.09	2.22	11.09
bar*	0.50	0.50	0.50
Efficiency*	0.75	0.75	0.75
Power (w)	205	41	205

TOTAL-Pumps Power Demand (w)	451.7
TOTAL-Pumps Power Density (W/m2)	10.8

Actual PRO only (W/m2)	**64.4**
Pumps Demand (W/m2)	-10.8
Turbine-Generator-10% PRO loss	-6.4
Net Electric Power (w/m2)	47.2

Energy per m3 Permeation (kWh/m3)	1.789
Energy per m3 LSF (kWh/m3)	0.895
Energy per m3 HSF (kWh/m3)	0.179

PRESSURE, NDP and FLUX DATA

Permeability Coefficient (l/m2/h/bar)			2.49
Module Parameters		Ideal	Actual
Type		NDP	FLUX	FLUX
	Applied -bar	bar	lmh	lmh

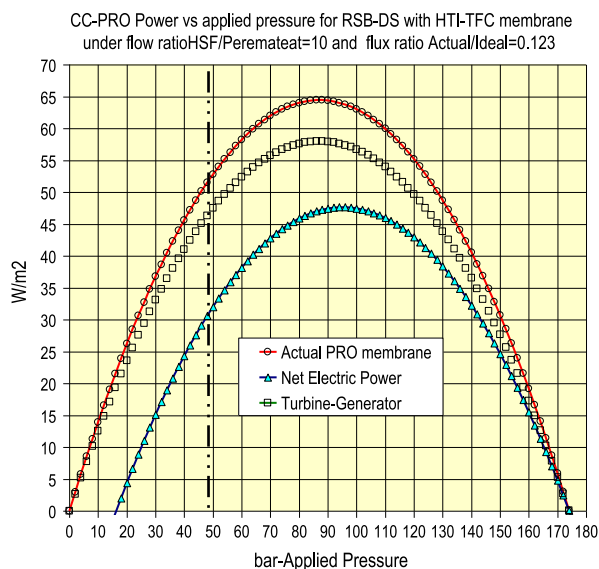|	Applied -bar	NDP bar	FLUX lmh (Ideal)	FLUX lmh (Actual)
Applied -bar	88.0			
Δπ MOD Inlet		215.0	127	316	39
Δπ MOD Outlet		133.2	45	113	14
Δπ MOD average		174.1	86.1	214.3	26.4
CC-PRO Selected average Flux				26.4

* Assumed

Fig. 4. Applied pressure vs actual power density of membrane, turbine-generator, and NEP availability projections for RSB–DS of ~220 bar osmotic pressure difference derived from the theoretical simulations of CC-PRO with HTI-TFC (A = 2.49 lmh/bar) under the stationary state conditions defined by β = 0.123, δ = 10, and α = 9.09% according to the database in Table 1.

CC-PRO is confined by the mechanical strength of membranes to withstand pressure and the vertical line in Fig. 4 illustrates the power availability of the HTI-TCF membrane at its maximum pressure limit of 48.3 bar where the power density of the membrane is 51.7 W/m² with turbine-generator equivalent of 46.6 W/m² and NEP availability of only 30.8 W/m².

4. Power generation prospects from RSB–DS using CC-PRO with HTI-TFC (A = 2.49 lmh/bar) at different flow ratio (δ = 1–25) under constant actual flux ratio (β = 0.123) conditions

The simulated NEP data in Table 2 for RSB–DS using CC-PRO with HTI-TFC and β = 0.123 as minimum are derived from the database in Table 1 with the appropriate δ values in the range 1–25, each pertaining to different stationary state conditions inside the PRO module. The data at the top part of the table entitled "Peak Pressure Projections" pertain to NEP peak and include the NEP density (W/m²); the NEP output of the entire unit (kW) accounting for the membrane surface area; the net specific energy output per permeation (kWh/m³); the net specific energy output per LSF (kWh/m³); the net specific energy output per HSF (kWh/m³); the RSB–DS annual power availability on the basis of the limiting RSB (LSF) projected flow to the DS; and the applied pressure of maximum

NEP. The data at the bottom part of the table entitled "Prospects at 48.3 bar applied pressure" pertain to the above-cited parameters at the pressure limit of the HTI-TFC membrane. The NEP curves as function of applied pressure under the selected flux ratio (β = 0.123) are displayed in Fig 5(A) for the flow ratio (δ) range 10–25 and in Fig. 5(B) for the flow ratio (δ) range 1–5. The dotted vertical lines in the figures intersect the NEP curves at the 48.3 bar limit of the HTI-TFC membrane. The data in Table 2 and Fig. 5(A) reveal declined NEP with increased peak pressure during the flow ratio (δ) change 10–25 and the data in Fig. 5(B) show increased NEP and peak pressure during the flow ratio (δ) change 1–5. According to the information provided in Table 2 and Fig. 5(A–B), maximum NEP availability with β = 0.123 takes place at δ = 10 with delivered electric power density of 47.7 W/m² and annual power prospects for a RSB–DS CC-PRO power station of 13,562 kW. Maximum NEP under the limiting pressure (48.3 bar) of the HTI-TFC membrane takes place at δ = 5 (34.8 W/m²) with 6,740 kW power availability from RSB–DS, however, maximum power availability of 7,753 kW takes place at δ = 1.0 (24.3 W/m²).

The projected performance of the CC-PRO unit with HTI-TFC membrane under constant flux ratio (β = 0.123) of different flow ratio (δ) revealed in Table 2 and Fig. 5 proceeds with some noteworthy trends created as function of the changing stationary state conditions inside the PRO module. Change of flow ratio (δ), made possible by CC-PRO through the flow rate selection of CP, creates the variations described in Fig. 6(A–D) of NEPD [A], NEP [B], and peak pressure [C] as well as the dependence of NEPD on applied pressure revealed in [D]. According to Fig. 6[A–D], maximum NEPD of 47.7 W/m² [A] and NEP of 2.003 kW [B] is reached at an applied pressure of 96 bar with δ = 10 yielding the highest maximum RSB–DS annual power availability of 13,562 kW (Table 2). If applied pressure is confined to 48.3 bar, the maximum NEPD (34.8 W/m²) and NEP (1.462 kW) are reached at δ = 5.0 with RSB-DS annual power availability of 6,740 kW, whereas, maximum annual power availability of 7.753 kW takes place at δ = 1.0. The specific energy contributions of the salinity gradient constituents as function of flow ratio to the energy production of the system under review are revealed for LSF [RSB] in Fig. 7(A) and for HSF [DS] in Fig. 7(B) with annual NEP availability from RSB–DS displayed in Fig. 8. Noteworthy is the resemblance of the curve pattern in Figs. 7(A) and 8 which is of no coincidence since the RSB [LSF] is the limiting source of the gradient and as such dictates the annual NEP availability of said salinity gradient. The data in Fig. 8 explain the annual NEP availability of 7.753 kW at 48.3 bar applied

Table 2
Minimum Net Electric Power generation prospects from RSB–DS using CC-PRO with HTI-TFC under constant $\beta = 0.123$ at different flow ratio (δ) in the range of 1–25

Net electric power parameters with constant actual/ideal flux ratio ($\beta = 0.123$)										
HSF/Permeate flow ratio	$\delta=$	25	20	15	10.0	5.0	2.5	2.0	1.5	1.0
Percent permeate in HSDF	$\alpha=$	3.85	4.76	6.25	9.09	16.67	28.57	33.33	40.00	50.00
Peak pressure prospects										
Net electric power density (W/m^2)		39.0	42.4	45.5	47.7	45.9	38.8	35.7	31.5	25.5
Net electric power of unit (kW)		*1.638*	*1.781*	*1.911*	*2.003*	*1.928*	*1.630*	*1.499*	*1.323*	*1.071*
Energy per m^3 permeation (kWh/m$^{3)}$		1.788	1.867	1.904	1.994	1.930	1.772	1.686	1.609	1.426
Energy per m^3 LSF (kWh/m^3)		0.894	0.933	0.965	0.990	0.965	0.886	0.843	0.804	0.713
Energy per m^3 HSF (kWh/m^3)		0.072	0.093	0.127	0.199	0.386	0.709	0.843	1.072	1.426
RSB–DS annual power availability (kW)[a]		*12,247*	*12,781*	*13,219*	*13,562*	*13,219*	*12,137*	*11,548*	*11,014*	*9,767*
Peak applied pressure (bar)		110	106	102	96	86	76	72	68	62
Prospects at 48.3 bar applied pressure										
Net electric power density (W/m^2)		10.0	17.3	24.4	30.8	34.8	32.8	31.2	28.6	24.3
Net electric power of unit (kW)		*0.420*	*0.727*	*1.025*	*1.294*	*1.462*	*1.378*	*1.310*	*1.201*	*1.021*
Energy per m^3 permeation (kWh/m^3)		0.245	0.430	0.615	0.801	0.984	1.078	1.097	1.117	1.132
Energy per m^3 LSF (kWh/m^3)		0.122	0.215	0.308	0.400	0.492	0.539	0.549	0.559	0.566
Energy per m^3 HSF (kWh/m^3)		0.010	0.022	0.041	0.080	0.197	0.431	0.549	0.745	1.132
RSB–DS annual power availability (kW)[a]		*1,671*	*2,945*	*4,219*	*5,479*	*6,740*	*7,384*	*7,521*	*7,658*	*7,753*

[a]Based on 120 Mm^3/year RSB disposed to DS.

pressure with $\delta = 1.0$ compared with the maximum of 13,562 kW attained with $\delta = 10$ at 96 bar applied pressure. The dependence of annual NEP availability from RSB–DS under constant $\beta = 0.123$ on applied pressure and flow ratio (δ) revealed in Fig. 9 shows the need of high enough applied pressure and flux ratio for effective power generation, whereas under fixed pressure (e.g., 48.3 bar) the availability is an inverse function of δ. In simple terms, the maximum power utility from the RSB–DS system under fixed applied pressure of 48.3 bar proceeds with low flow ratio which also manifests the lower flow rate requirements of the auxiliary pumps CP, HSF-P, and LSF-P and the need for conduit lines of smaller diameters. The data in Fig. 9 also imply that if the mechanical strength the HTI-TFC membrane could be enhanced to withstand 86 bar applied pressure, the NEP availability will exceed 13,000 kW.

5. Power generation prospects from RSB–DS using CC-PRO with HTI-TFC (A = 2.49 lmh/bar) at different flux ratio (β = 0.123 → 0.40) under constant flow ratio (δ = 5 conditions)

The selection of $\beta = 0.123$ as minimum for the HTI-TFC membrane in the context of CC-PRO power generation from RSB–DS is suggested by the well-documented behaviors of this membrane in 0.6–3.0 M NaCl gradients. CC-PRO power projections with

$\beta = 0.123$ should be viewed as a minimum reference level with actual projection expected to be higher, or even much higher, in light of the presence of relatively large amounts of divalent ions in DS of lower reverse salt flux characteristics compared with sodium. In light of the aforementioned, it is found of interest to ascertain the CC-PRO performance of the HTI-TFC membrane over a wider range of flux ratio and the results of such simulations for the flow ratio $\delta = 5.0$ and β range 0.123–0.400 are summarized in Table 3 with NEPD projections as function of applied pressure displayed in Fig. 10. The focus on the flow ratio $\delta = 5.0$ in this table is of no coincidence since the stationary state conditions inside the PRO module created at this particular flow ratio are of near maximum power prospects at a reasonable applied pressure of about 86 bar according to the data presented in Table 2, Fig. 6(A–D), Figs. 7(A), 8, and 9. The stationary state conditions prevailing inside the PRO module at flow ratio $\delta = 5.0$ should allow maximum NEPD at the same peak pressure (86 bar) irrespective of flux ratio with increased β (0.123–0.40) concomitant with increase NEPD (45.9–149 W/m^2) and power output of unit (1.928–6.271 kW per module). Flow rates and osmotic pressure differences at module inlet and outlet remain essentially unchanged at the same flow ratio and therefore, the PRO specific energy constituents (kWh/m^3) of permeation, LSF and HSF are unaffected
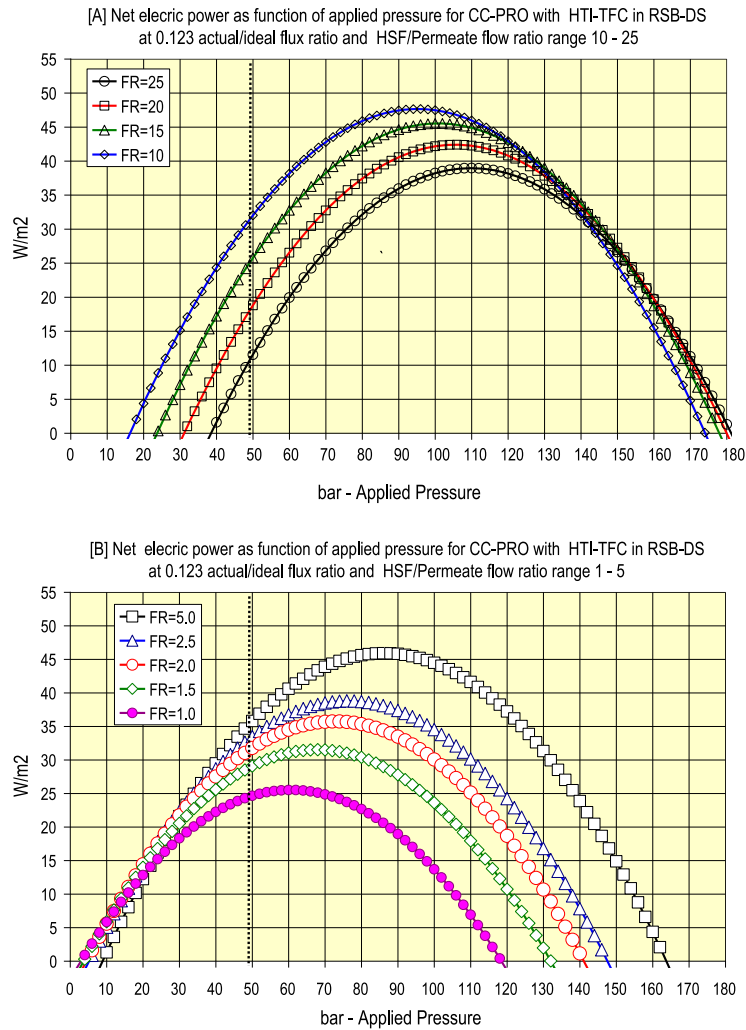
Fig. 5 (A–B). Minimum NEPD prospects as function of applied pressure from RSB–DS using CC-PRO with HTI-TFC under constant flux ratio ($\beta = 0.123$) in the flow ratio (δ) ranges 10–25 (A) and 1–5 (B).

by change of β since more energy is associated with higher flow rates and vice versa. Maximum power availability from RSB–DS is a function of the limiting salinity source, or RSB in this instance, and derived from the product of the LSF specific energy and its annually consumed volume. For instance, LSF specific energy of 1.930kWh/m³ combined with 120 Mm³/year RSB expected in the Jordanian RS–DS pilot project represent an annual NEP availability of 13,219 kW (120x10⁶x0.965/365/24). Declined NEPD toward a lower applied pressure from the maximum illustrated in Fig. 10 together with unchanged flow rates inside the PRO module at the same flow ratio (e.g. $\delta = 5.0$ in Fig. 10) dictate lower LSF specific energy and consequently, a lower NEP availability from the RSB–DS CC-PRO plant as function of the applied pressure of

operation. The LSF specific energy at peak pressure of 86 bar (0.965 kWh/m³) and at the membrane pressure limit of 48.3 bar (0.493 kWh/m³) exemplified in Table 3 appear to be essentially independent on flux ratio with decreased NEP availability (13,200–6,750 kW, respectively) manifesting a change of applied pressure.

6. Discussion

The RS–DS water transfer (200 Mm³/y) pilot project sponsored by the Word Bank to be followed eventually by a 10-fold major program is intended to stop the rapidly declined sea level of the DS, provide fresh water (80 Mm³/y) through seawater desalination to arid zones, and generate hydroelectric power due to the 400 m level difference between these water sources.
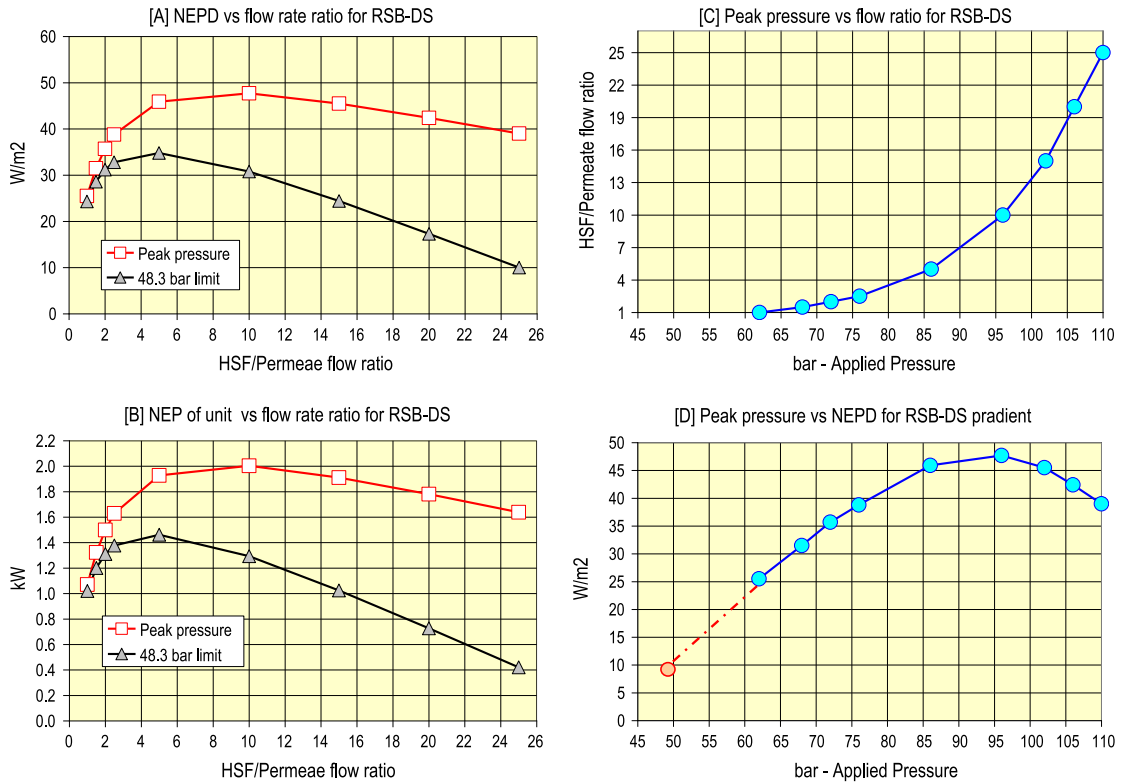
Fig. 6 (A–D). Flow ratio effects on NEPD (A), NEP (B), and applied pressure peak (C) as well as the dependence of NEPD on maximum applied pressure (D) for RSB–DS using CC-PRO with HTI-TFC under the constant flux ratio $\beta = 0.123$.
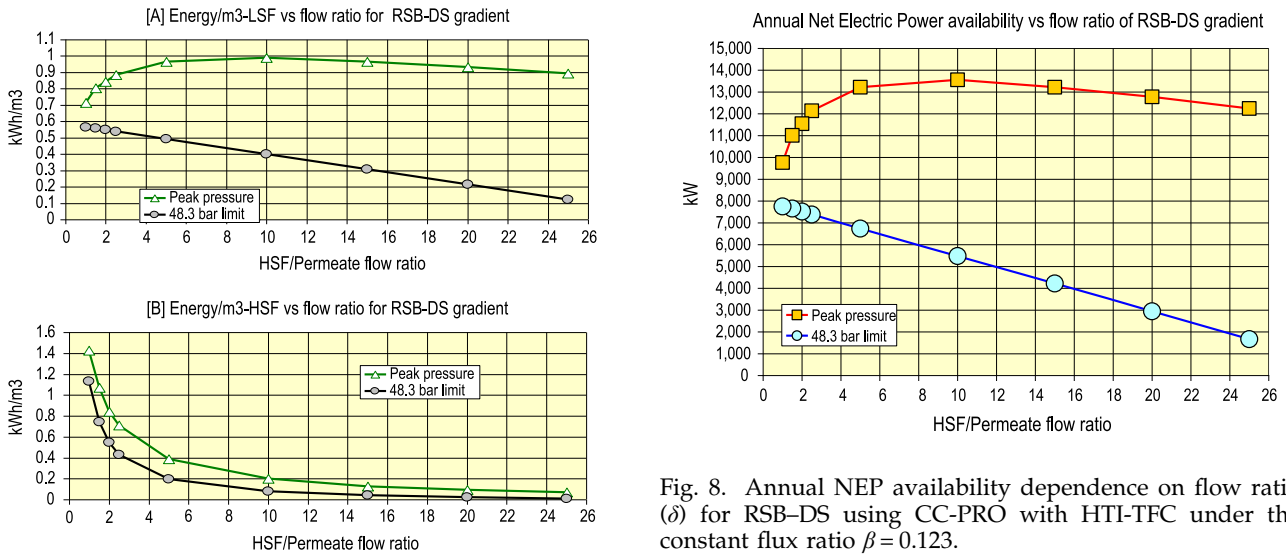

Fig. 7 (A–B). Flow ratio effects on the specific energy contribution of LSF (A) and HSF (B) for RSB–DS using CC-PRO with HTI-TFC under the constant flux ratio $\beta = 0.123$.

Fig. 8. Annual NEP availability dependence on flow ratio (δ) for RSB–DS using CC-PRO with HTI-TFC under the constant flux ratio $\beta = 0.123$.

This project and the ultimate program will generate large amounts of RSB (120 Mm³/y initially and 1,200 Mm³/y ultimately) on the shores of the DS which could

be used for PRO hydroelectric power generation and this study explores the current and future prospects for clean energy production by CC-PRO as an added benefit to the RS–DS water transfer pilot and program.

The power generation prospects from RSB–DS are ascertained through the use of the CC-PRO
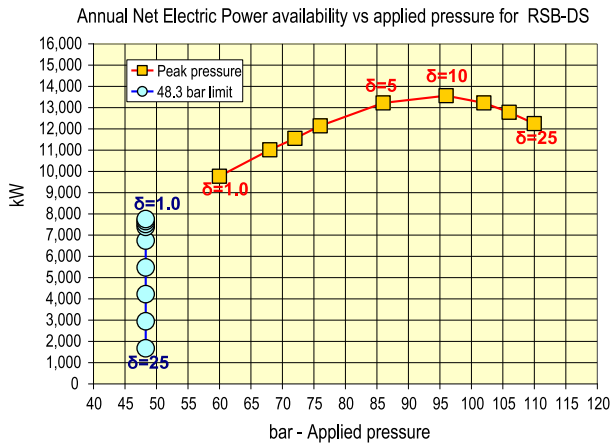
Fig. 9. Annual NEP availability dependence on applied pressure and flow ratio (δ) for RSB–DS using CC-PRO with HTI-TFC under the constant flux ratio $\beta = 0.123$.

technology of near absolute energy efficiency without need of ERD with a recently reported PRO-TFC membrane (HTI-TFC) of the highest reported [32] mechanical strength to withstand pressures up to 700 psi (48.3 bar). The expected RSB (LSF) constituent (7.13%) in the process will be derived from a low recovery (40%) desalination plant of RS water (4.28%) and therefore, of sufficiently high quality without need for pretreatment. The ratio for RSB utility of LSC/LSF = 0.50 in the process under review is selected to avoid scaling of calcium sulfate in the low pressure section of the model apparatus (Fig. 1). The presence of only minor amount of sulfate (0.2%) in DS water precludes the possibility of calcium sulfate scaling on either sides of the semi-permeable membrane during the

process and/or after the disposing HSC effluent to the DS. The operational conditions of CC-PRO with HTI-TFC for RSB–DS are carefully analyzed in this study with respect to the flux ratio (β) of the membrane and the stationary state conditions inside the PRO module as function of flow ratio (β) for the best power generation prospects. On the basis of the β-A power performance criteria of the HTI-TFC membrane in 0.6–3.0 M NaCl gradients and its expected performance with DS water of relatively high concentrations of calcium (5.1%) and magnesium (12.9%), the $\beta = 0.123$ used in the RSB–DS CC-PRO simulation is most obviously a minimum with actual β expected to be found significantly higher for reasons associated with PRO reduced reverse salt diffusion of divalent ion through semi-permeable membranes in PRO. The minimum power projections for RSB–DS using CC-PRO with HTI-TFC of $\beta = 0.123$ over the flow ratio range (δ) 1–25 are presented in Table 2 and Figs. 5–9 and reveal maximum NEPD and NEP at $\delta = 10$ and the best stationary state of reasonable applied pressure (86 bar) association with $\delta = 5$. Power projections for the system under review with $\delta = 5$ over the flux ratio (β) range 0.125–0.400 are presented in Table 3 and Fig. 10 with realistic HTI-TFC performance expected over the flux ratio range 0.20–0.25 instead of the 0.123 minimum.

Interpretation of the extensive analysis data presented hereinabove in context of CC-PRO feasibility for RSB–DS application is summarized in Table 4 in terms of the best NEP availability on the basis of the limiting RSB (HSF) salinity source at the level of the HTI-TFC membrane of 48.3 bar maximum applied pressure limitation and future membrane alike with
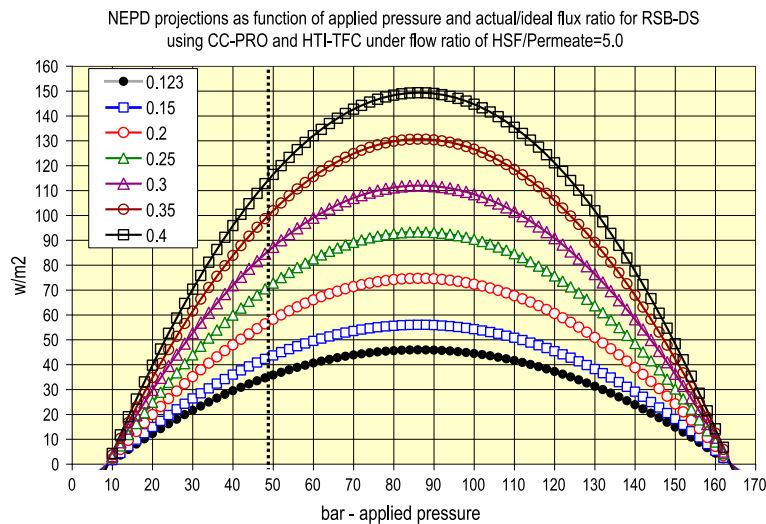

Fig. 10. NEPD projections as function of applied pressure for RSB–DS using CC-PRO with HTI-TFC under the constant flow ratio of $\delta = 5.0$ at different flux ratio ($\beta = 0.123$–0.400).

Table 3
NEPD projections at different flux ratios (β = 0.123–0.400) for RSB–DS using CC-PRO with HTI-TFC under the constant flow ratio of δ = 5.0 generated by the simulation database displayed in Table 1 with the appropriate β and δ terms

Net electric power parameters for flow ratio HSF/permeate = 5.0							
Actual/ideal flux ratio selection β=	0.123	0.150	0.200	0.250	0.300	0.350	0.400
Peak at 86 bar applied pressure							
Net electric power density (W/m²)	45.9	56.0	74.7	93.3	111.9	130.7	149.3
Net electric power of unit (kW)	*1.928*	*2.352*	*3.137*	*3.919*	*4.700*	*5.489*	*6.271*
Energy per m³ permeation (kWh/m³)	1.930	1.931	1.930	1.928	1.987	1.927	1.927
Energy per m³ LSF (kWh/m³)	0.965	0.966	0.965	0.964	0.965	0.964	0.963
Energy per m3 HSF (kWh/m³)	0.386	0.386	0.386	0.386	0.385	0.385	0.385
RSB–DS annual power availability (kW)[a]	*13,219*	*13,233*	*13,219*	*13,205*	*13,219*	*13,205*	*13,192*
Applied pressure of 48.3 bar							
Net electric power density (W/m²)	34.8	42.5	56.7	70.8	85.0	99.2	113.3
Net Electric Power of unit (kW)	*1.462*	*1.785*	*2.381*	*2.974*	*3.570*	*4.166*	*4.759*
Energy per m³ permeation (kWh/mm³)	0.984	0.986	0.985	0.985	0.985	0.986	0.985
Energy per m3 LSF (kWh/m³)	0.492	0.493	0.493	0.492	0.492	0.493	0.493
Energy per m3 HSF (kWh/mm³)	0.197	0.197	0.197	0.197	0.197	0.197	0.197
RSB–DS annual power availability (kW)[a]	*6,740*	*6,753*	*6,753*	*6,740*	*6,740*	*6,753*	*6,753*

[a]Based on disposing 120 Mm3/year of RSB to the DS.

sufficient mechanical strength to operate at 60 bar or even 86 bar applied pressure. NEP availability of each of the pressure categories is presented as minimum with β = 0.123 and as a realistic projection with β = 0.200 with actual maximum could reach an even higher value. Noteworthy information revealed in Table 4 pertains to immediate availability of CC-PRO with HTI-TFC at 48.3 bar applied pressure for RSB–DS NEP generation of considerable output (6,740 –7,753 kW) with difference between β of 0.123 and 0.200 manifested the number of modules required in the PRO plant – proportionally less modules are required by increased β. The table also provides a forecast for the near future and future by assuming that the specific membrane under review, or alike, could be made to operate at 60 bar and 86 bar applied pressure, respectively, instead of the current limit of 48.3 bar.

The data in this study focuses on the NEPD and NEP generation prospects from RSB–DS using HTI-TFC after accounting for the power demand of the auxiliary pumps and the efficiency of the turbine-generator unit and this in order to facilitate the economic evaluation of system under review. The size of a modular CC-PRO apparatus/plant is determined by the number of parallel modules with their inlets and outlets connected in parallel to the same closed circuit with its side conduits and circulation means. The side conduits comprise expanded pipe section with valve means to enable their engagement/disengagement with the closed circuit and the auxiliary pumps in the

design are of low power demand since they are intended for low pressure difference operation. Combination of CC-PRO operation of near absolute energy efficiency without need of ERD with auxiliary pumps of low power consumption should lead to high NEPD and NEP output of low installation cost not possible by the conventional PRO technique with ERD means. The tentative cost estimates in Table 4 assume 20$ per m² membrane surface with cost of membranes manifesting 35% of the total installation cost of the plant. The cost figures in the table clearly reflect the performance characteristics of the membrane with higher β inversely proportional to installation cost. The realistic cost figures in the table are those associated with β = 0.200. The CC-PRO technology performance with HTI-TFC membranes of 48.3 bar applied pressure limit suggests an immediate process availability of high feasibility for economic hydroelectric power generation from the RSB–DS salinity gradient at the level of 6,740–7,753 kW depending on the specific β and δ parameters selection. Near future expected developments of HTI-TFC or membranes, alike, to withstand pressure of 60 bar will enable the increased power availability from RSB–DS to 9,767 kW with a further increase to 13,219 kW expected when such membranes could be made to operated at 86 bar with each increased capacity associated with decreased specific installation costs. The projections made hereinabove specifically in the context of DS surface water as HSF (draw) in conjunction with RS-derived RSB brine as LSF should ultimately

Table 4
Present NEP generation prospects from RSB–DS using CC-PRO with HTI-TFC membrane of $\beta = 0.123$ (low estimate) and $\beta = 0.200$ (realistic estimate) at 48.3 bar applied pressure as well as near future (60 bar) and future (86 bar) projections assuming that the cited membrane, or alike, could be made to withstand the indicated pressures in parenthesis

Membrane characteristics			CC-PRO HTI-tfc process parameters					RSB–DS CC-PRO HTI-TFC power plant				
Coeff. (A) lmh/	Flux (β)	Allowed Press.	Flow (δ)	Applied Press.	RSB (LSF)	PRO Module[a] NEPD	NEP[a]	Plant NEP[b]	Plant Modules	Specific Cost[c]	Plant Cost	availability
bar	ratio	bar	ratio	bar	kWh/ m3	W/ m2	kW	kW	No	$/kW	$	STATUS
2.49	0.123	86.0	5.0	86.0	0.965	45.9	1.928	13,219	6,856	1,246	16,471,642	Future
2.49	0.200	86.0	5.0	86.0	0.965	74.7	3.137	13,219	4,214	766	10,123,470	Future
2.49	0.123	48.3	5.0	48.3	0.492	34.8	1.462	6,740	4,610	1,643	11,075,360	Immediate
2.49	0.200	48.3	5.0	48.3	0.493	56.7	2.381	6,753	2,836	1,009	6,813,695	Immediate
2.49	0.123	60.0	1.0	60.0	0.713	25.5	1.071	9,767	9,120	2,243	21,908,722	near future
2.49	0.200	60.0	1.0	60.0	0.713	41.5	1.743	9,767	5,604	1,378	13,461,986	near future
2.49	0.123	48.3	1.0	48.3	0.566	24.3	1.021	7,753	7,594	2,353	18,242,710	Immediate
2.49	0.200	48.3	1.0	48.3	0.566	39.5	1.659	7,753	4,673	1,448	11,227,129	Immediate

[a]NEP per module of 42 m^2 membrane surface area.
[b]NEP per plant with indicated number of PRO modules for maximum utility of the RSB as HSF source.
[c]Specfiic installation cost : 20 $/m^2 per membrane with membranes account for 35% of the total cost.

resolve the question raised by Loeb [5] with regards to "*Energy production at the Dead Sea by pressure-retarded osmosis: challenge or chimera?*".

Hydroelectric power in the RS–DS water transfer project originates from the ~400 m height difference between the desalination plant and the DS shores, and the disposing of 120 Mm^3/y (13,698 m^3/h) RSB at ~40 bar pressure translates to 13,698 kW hydroelectric power generation with assumed turbine-generator efficiency of 90%. The data in Table 4 reveal that the CC-PRO technology with HTI-TFC membrane, both of immediate availability, could provide 7,753 kW or 56.6% power supplement to the Jordanian project just by utilizing the brine effluent entry to the DS. The power supplement will grow to 71.3% and 96.5% when said membrane, or alike, could be made to operate at the respective pressure of 60 bar and 86 bar and such developments are expected within the next few year and most probably even before the commissioning of RS–DS project. The afore cited major power supplements through CC-PRO and HTI-TFC for the RS–DS project are created on the shores of the DS just before the entry of the RSB effluent without link and/or adverse effect on any

aspect of the project and the adding of this feature to the project can take place after its commissioning.

Conventional PRO is distinguished from CC-PRO by its ERD and the effectiveness of such devices in the PRO demonstration units operated in Norway [33−35] and Japan [36−38] was never disclosed despite the crucible role played ERD in the process. Modern SWRO desalination plant heavily rely on ERD for saving of energy, however, reported [40] RO specific energy data of such plants consistently revealed energy conversion efficiency around 75% or less with a typical example reported [39] for the Palmachim Plant (Israel) where the energy conversion efficiency is found "*just over 76% at the best efficiency point*" and less below the referred point. In contrast with SWRO where energy recovery takes place from the pressurized brine flow which is approximately half of the pressurized feed flow, energy recovery in conventional PRO implicates the entire HSF intake flow and this implies an even greater dependence on the efficiency of ERD for energy conservation. Accordingly, conventional PRO with ERD is unlikely proceeded with high enough energy conversions efficiency of economical

feasibility as expected with the CC-PRO technology of near absolute energy efficiency prospects.

6. Concluding remarks and summary

The Red Sea (RS) to Dead Sea (DS) water transfer project in Jordan under the sponsorship of the World Bank is intended to stop the sea-level decline of the DS as well as for the desalination of RS water and for hydroelectric power generation. Red Sea Brine (RSB ~7.13%) disposal to the DS (~34%) creates a salinity gradient of interest for PRO hydroelectric power generation and the prospects of such an application are explored in the present study with the most advanced existing tools including a new Closed Circuit PRO technology (CC-PRO) of near absolute energy efficiency without need of ERD and a recent PRO membrane (HTI-TFC) of the highest reported strength to withstand applied pressure up to 48.3 bar. Power generation prospects from RSB–DS using CC-PRO with HTI-TFC are assessed in the actual/ideal flux ratio (β) range 0.123–0.400 and High Salinity Feed (DS as draw solution) to permeation flow ratio (δ) range 1–25. The minimum $\beta = 0.123$ for said process is established from available PRO experimental data with HTI-TFC for 0.6–3.0 M NaCl salinity gradients accounting for the presence of considerable concentrations of divalent ions such as Ca and Mg in DS water. The NEP generation prospects from the RSB–DS Jordanian project using CC-PRO and HTI-TFC are assessed on the basis of 120 Mm^3/year RSB availability for mixing with DS water.

The results of this study accounting for the pressure limitation of HTI-TFC reveal Net Electric Power (NEP) generation prospects of 7,753 kW under the conditions of $\delta = 1.0$ and $\beta = 0.123$–0.200 from the RSB–DS gradient, or a supplement of 56.6% more power on top of the conventional hydroelectric power generation facility of the project (~13,698 kW). If the HTI-TFC membrane, or alike, could be made to operate at maximum PRO pressures of 60 and 86 bar, the CC-PRO NEP availability from RSB–DS is expected to rise to 9,767 kW (71.3%) and 13,219 kW (96.5%), respectively, with added power to the project indicated in parenthesis. In simple terms, the current state of the art revealed in this study suggests the immediate availability of the CC-PRO technology with HTI-TFC membranes for economical NEP generation from the RSB–DS gradient in the context of the Jordanian project with future improvements of membranes to withstand higher applied pressures expected to improve the economic feasibility.

References

[1] S. Loeb, Method and apparatus for generating power utilizing pressure-retarded-osmosis. US patent No 3,906,250, 1975.
[2] S. Loeb, R.S. Norman, Osmotic –Power Plants, Science 189 (1975) 654–655.
[3] S. Loeb, Production of energy from concentrated brined by pressure-retarded osmosis, preliminary technical and economic correlations, J. Mem. Sci. 1 (1976) 49–63.
[4] S. Loeb, F. van Hessen, D. Shahaf, Production of energy from concentrated brine by pressure-retarded osmosis: II Experimental results and projected energy costs, J. Mem. Sci. 1 (1976) 249–269.
[5] S. Loeb, Energy production at the Dead Sea by pressure-retarded osmosis: challenge or chimera? Desalination 120 (1998) 247–262.
[6] S. Loeb, S. Sourirajan, American Chemical Society Advances in Chemistry Series, ACS 38 (1963) 117–132 and references therein.
[7] A. Achilli, T.Y. Cath, A.E. Childress, Power generation with pressure retarded osmosis: An experimental and theoretical investigation, J. Mem. Sci. 343 (2009) 42–52.
[8] A. Achilli, T.Y. Cath, A.E. Childress, Selection of inorganic-based draw solutions for forward osmosis applications, J. Mem. Sci. 364 (2010) 233–241.
[9] A. Achilli, A.E. Childress, Pressure Retarded Osmosis: From the vision of Sidney Loeb to the first prototype installation – Review, Desalination 261 (2010) 205–211.
[10] M. Elimelech, W.A. Phillip, The future of seawater desalination: Energy, technology, and the environment, Science 333 (2011) 712–717 and references therein.
[11] B.E. Logan, M. Elimelech, Membrane-based processes for sustainable power generation using water, Nature 488 (2012) 313–319 and references therein.
[12] S.J. Duraneau, Emergence of Forward Osmosis and Pressure Retarded Osmosis Process for Drinking Water Treatment. Florida Water Res. J July (2012) 32–36.
[13] X. Wanga, Z. Huanga, L. Lib, S. Huangc, E.H. Yud, K. Scott, Energy generation from osmotic pressure difference between the low and high salinity water by pressure retarded osmosis, J. Technol. Innovations Renewable Energy 1 (2012) 122–130.
[14] T.-S. Chung, X. Li, R.C. Ong, Q. Ge, H. Wang, G. Han, Emerging forward osmosis (FO) technologies and challenges ahead for clean water and clean energy applications, Curr. Opin. Chem. Eng. 1 (2012) 246–257.
[15] L. Checkli, S. Phuntsho, H.K. Shon, S. Vigneswaran, J. Kandasamy, A. Chahan, A review of draw solutes in forward osmosis process and their use in modern applications, Desalin. Water Treat. 43 (2012) 167–184.

[16] Inger Lise Alsvik, May-Britt Hägg, Pressure retarded osmosis and forward osmosis membranes, Polymers 5 (2013) 303–327.

[17] Florian Dinger, Tobias Tröndle, Ulrich Platt, Optimization of the energy output of osmotic power plants. J. Renewable Energy (2013) 7.Available from: http://dx.doi.org/10.1155/2013/496768 (Article ID 496768).

[18] C. Klaysom, T.Y. Cath, T. Depuydt, F.J. Ivo Vankelecom, Forward and Pressure retarded osmosis: potential solutions for global challenges in energy and water Supply, Chem. Soc. Rev 42 (2013) 6959–6989.

[19] M. Sabah, A.F. Atwan, H.B. Mahood, A. Sahrif, Power generation based on pressure retarded osmosis : A design and an optimization study, Int. J. Appl. Eng. Manage 2(12) (2013) 68–74.

[20] F. Dinger, T. Trondle, U. Platt, Optimization of the Energy Output of Osmotic Power Plants, J. Renewable Energy (2013) 7 (Article ID 496768).

[21] J.R. McCutcheon, M. Elimelech, Influence of membrane support layer hydrophobicity on water flux in osmoticaly driven membrane process, J. Membr. Sci. 318 (2008) 458–466.

[22] N.Y. Yip, A. Tiraferri, W.A. Phillip, J.D. Schiffman, M. Elimelech, Performance thin-film composite forward osmosis membrane, Environ. Sci. Technol 44 (2010) 3812–3818.

[23] N.Y. Yip, M. Elimelech, Performance limiting effects in power generation from salinity gradients by pressure retarded osmosis, Environ. Sci. Technol. 45 (2011) 10273–10282.

[24] N.Y. Yip, A. Tiraferri, W.A. Phillip, J.D. Schiffman, L.A. Hoover, Y.C. Kim, M. Elimelech, Thin-film composite pressure retarded osmosis membranes for sustainable power generation from salinity gradients, Environ. Sci. Technol. 45 (2011) 4360–4369.

[25] N.Y. Yip, A. Tiraferri, W.A. Phillip, J.D. Schiffman, L.A. Hoover, Y.C. Kim, M. Elimelech, Thin-film composite pressure retarded osmosis membranes for sustainable power generation from salinity gradients, Environ. Sci. Technol 45 (2011) 4360–4369.

[26] S. Chou, R. Wang, L. Shi, Q. She, C. Tang, A.G. Fane, Thin-film hollow fiber membrane for pressure retarded osmosis (PRP) process with high power density, J. Mem. Sci. 389 (2012) 25–33.

[27] S. Zhang, T.S. Chung, Minimizing the instant and accumulation effects of salt permeability to sustain ultrahigh osmotic power density", S. Zhang and T.S. Chung, Environ. Sci. Technol. 47 (2013) 10085–10092.

[28] S. Zhang, F. Fu, T.S. Chung, Substrate modified and alcohol treatment on this film composite membranes for osmotic power, Chem. Ing. Sci. 87 (2013) 40–50.

[29] X. Li, S. Zhang, F. Fu, T.S. Chung, Deformation and reinforcement of thin-film composite (TFC) polyamide-imide (PAI) membranes for osmotic power generation, J. Mem. Sci 434 (2013) 204–217.

[30] G. Han, S. Zhang, X. Li, T.S. Chung, High performance thin film composite pressure retarded osmosis (PRO) membranes for renewable salinity – gradient energy generation, J. Mem. Sci. 440 (2013) 108–121.

[31] X. Song, Z. Liu, D.D. Sun, Energy recovery from concentrated seawater brine by a thin-film nanofiber composite pressure retarded osmosis membranes with high power density, Energy Environ. Sci. 6 (2013) 1199–1210.

[32] A.P. Straub, N.Y. Yip, M. Elimelech, Raised the bar: Increased hydraulic pressure enables unprecedented high power density in pressure retarded osmosis, Environ. Sci. Technol. Lett 1(1) (2014) 55–59.

[33] S.E. Skilhagen, J.E. Dugstad, R.J. Aaberg, Osmostic power – power production based on the osmotic pressure difference between waters and varying salt gradients, Desalination 220 (2008) 476–482.

[34] S.E. Skilhagen, G. Brekke, W.K. Nielsen, Progress in the Development of Osmotic Power, 2011 Qingdao International Conference on Desalination and Water Reuse, Proceedings 247–260, June 20–23, 2011 Qingdao, China.

[35] G. Brekke, Review of experience with the Statkraft prototype plant, The 3rd Osmosis Membrane Summit, April 26–27 (2012), Barcelona, Spain.

[36] A. Tanioka, Power generation by pressure retarded osmosis using concentrated brine from seawater desalination system and treated sewage, review of experience with pilot in Japan, The 3rd Osmosis Membrane Summit, April 26–27, 2012, Barcelona, Spain, 2012.

[37] M. Kurihara, Government funded programs worldwide, the Japanese "Mega-ton Water System" project, The 3rd Osmosis Membrane Summit, April 26–27, 2012, Barcelona, Spain.

[38] K. Saito, M. Irie, S. Zaitsu, H. Sakai, H. Hayashi, A. Tanioka, Retarded osmosis using concentrated brine from SWRO system and treated sewage as pure water, Desalin. Water Treat. 41(3) (2012) 114–121. 4.

[39] A. Hermoni, Actual Energy Consumption and Water Cost for the SWRO Systems at Palmachim – Case History", IDA conference, November 2–3, 2010, CA, US.

[40] A. Efraty, Closed circuit desalination series no-6: conventional RO compared with the conceptually different new closed circuit desalination technology, Desalin. Water Treat. 41 (2012) 279–295.

[41] PCT Patent Application, Power generation by pressure retarded osmosis in closed circuit without need of energy recovery, International Publication Number WO 2012/140659 A1, 18 October 2012, inventor – Avi Efraty.

[42] A. Efraty, Closed circuit pressure retarded osmosis – A new technology for clean power generation without need of energy recovery, The 3rd Osmosis Membrane Summit, April 26–27, 2012, Barcelona, Spain.

[43] A. Efraty, Pressure-retarded osmosis in closed circuit: a new technology for clean power generation without need of energy recovery, Desalin. Water Treat. 51 (2013) 7420–7430.

[44] http://wikipeida.org/wiki/Red_Sea%E2%80%93Dead_Sea_Canal and references therein describing the Red-Sea Dead-Sea designed Canal – The pilot program was singed at the World-Band office in Washington DC, US in the beginning of December, 2013.

[45] Hydration Technology Innovations, HTI, Albany, NY, US Available from: http://www.htisater/

[46] A. Efarty, Closed circuit PRO Series No 2: Performance projections for PRO membranes by a simple approach base on actual/ideal flux ratio at zero applied pressure. 2014 (submitted for publication).